CrystEngComm

PAPER

View Article Online
View Journal | View Issue

Cite this: *CrystEngComm*, 2015, **17**, 2406

Received 26th December 2014,
Accepted 4th February 2015

DOI: 10.1039/c4ce02538e

www.rsc.org/crystengcomm

Growth of silica nanowires in vacuum

V. Gurylev,[a] C. C. Wang,[b] Y. C. Hsueh[a] and T. P. Perng*[a]

Silica nanowires were grown on a Pt-coated Si substrate in flowing Ar, dynamic vacuum, and sealed vacuum tubes. The amount of oxygen in the reaction chamber or tubes directly influenced the composition and morphology of the nanowires. The formation of nanowires assisted by Pt can be explained by the VLS mechanism and active oxidation of silicon. In flowing Ar and dynamic vacuum, the dimensions of the nanowires increased with the partial pressure of oxygen. For nanowires grown in sealed tubes, the nanowires became much shorter which can be ascribed to the limited amount of residual oxygen in the tube. Therefore, the growth of silica nanowires is determined by a critical concentration of oxygen, below which the growth of nanowires is suspended.

Introduction

In the past several years, silica (SiO_x) nanowires have attracted immense interest due to their excellent electronic and optical properties.[1–3] The ability to produce silica nanowires in a controlled manner is crucial for device applications. Various approaches, such as laser ablation,[4] oxide-assisted growth,[5] sol–gel template method,[6] carbothermal reduction,[7] and gas-phase and surface diffusion growth (including vapor–liquid–solid (VLS), vapor–solid (VS), and solid–liquid–solid (SLS) processes),[8] have been explored to synthesize silica nanowires.

Among these methods, the VLS process has been proven to be more reliable for localized nucleation of silica nanowires. This process was first suggested by Wagner and Ellis in 1964, who observed that micrometer-scale silicon whiskers (wires) could be grown *via* decomposition of gaseous precursors (SiH_4 or SiH_2Cl_2) by means of a nanosized liquid alloy droplet catalyst which was initially introduced in the form of metallic thin films or nanoparticles.[9] However, the presence of a toxic silicon gas source makes this process unsafe and rather complicated. Instead, it was recently discovered that amorphous silica nanowires could be grown by using a relatively simple technique based on the annealing of a silicon substrate covered with a metal catalyst in inert atmosphere (*e.g.*, N_2 or Ar) at temperatures close to 1100 °C.[10–15] The presence of a particle on the tip of a nanowire was attributed to the VLS mechanism. It was noticed that the silicon source was supplied by decomposition/diffusion or evaporation of the silicon substrate,[12,16] and the presence of SiO_x species, as the dominant vapor phase component, was responsible for the concrete growth of nanowires.[17–20] The source of oxygen usually comes from the decomposition of native oxide, impurities in the gas atmosphere, or leakage.[21,22]

The experimental procedures reported in the literature usually include the necessary purging of the reaction chamber with an inert gas. It has been reported, except for a few studies,[23,24] that the growth of silica nanowires could not proceed by any means in vacuum, whether dynamic (*i.e.*, with residual gas flow) or sealed (*i.e.*, without gas flow). Moreover, it has been demonstrated that there is a critical value of the inert gas flow rate below which the growth of nanowires could not be promoted.[18]

The present study will discuss the influence of the gas environment on the growth of silica nanowires and demonstrate that the nanowires, despite the generally accepted conclusion, can be successfully produced in vacuum with and without air flow. Furthermore, it will be evidenced that the growth, composition, and final morphology of the silica nanowires are dependent on the concentration of oxygen in the reaction chamber, which can be controlled by the degree of vacuum. The general theory for the growth of silica nanowires, based on the present experimental results, will also be discussed in detail.

Experimental

An n-type silicon wafer (100) was used as a substrate material for deposition of Pt nanoparticles (NPs). The substrate was immersed in a solution of H_2SO_4 and H_2O_2 (ratio 3 : 1) for 3 min to remove contaminants. Platinum nanoparticles were deposited on the surface of the silicon substrate by plasma-enhanced atomic layer deposition (PEALD). The substrate temperature was set at 300 °C, and the power of the plasma source was 100 W. $MeCpPtMe_3$ was used as a precursor of Pt. The duration of pulse time was 0.1 s for the Pt precursor, 5 s

[a] *Department of Materials Science and Engineering, National Tsing Hua University, Hsinchu 300, Taiwan. E-mail: tpperng@mx.nthu.edu.tw; Fax: +886 3 5723857; Tel: +886 3 5742634*
[b] *Department of Materials Science and Engineering, Feng Chia University, Taichung 407, Taiwan*

for O_2/Ar plasma, and 5 s for nitrogen flow. The pressure of the O_2/Ar plasma source was held at 1.5/0.5 torr. The vacuum in the chamber was controlled at 10^{-3} torr. The total number of cycles for the PEALD process was 100.

After the deposition of Pt NPs was finished, the silicon substrate was immediately transferred into a furnace for thermal treatment or directly sealed in a quartz tube (diameter 2.4 cm, length 6.0 cm) under vacuum. The thermal treatment in the furnace was carried out to synthesize silica nanowires at 1000 °C for 1 h in an argon flow or in a dynamic vacuum at 10^{-3} torr. Additionally, three levels of vacuum (10^{-3} torr, 10^{-2} torr, and 10^{-1} torr) were maintained inside the sealed quartz tube, and the samples were also subjected to thermal treatment at 1000 °C for 1 h.

Results and discussion

3.1. Thermal treatment in argon

Fig. 1(a) shows the SEM image of the silica nanowires grown in argon atmosphere at 1000 °C for 1 h. It is clear that the as-grown nanowires are twisted and interwoven together. The average diameter of the nanowires is 60–70 nm and the length is over 100 μm. The TEM micrograph in Fig. 2(a) shows the higher magnification image of the nanowires. There is a particle on the tip of each nanowire, as also shown in the inset of Fig. 1(a), which can be attributed to VLS growth. X-ray diffraction (XRD) analysis (Fig. 3(a)) reveals the amorphous nature of the nanowires, except for the peaks ascribed to PtSi on the tip of the nanowires.

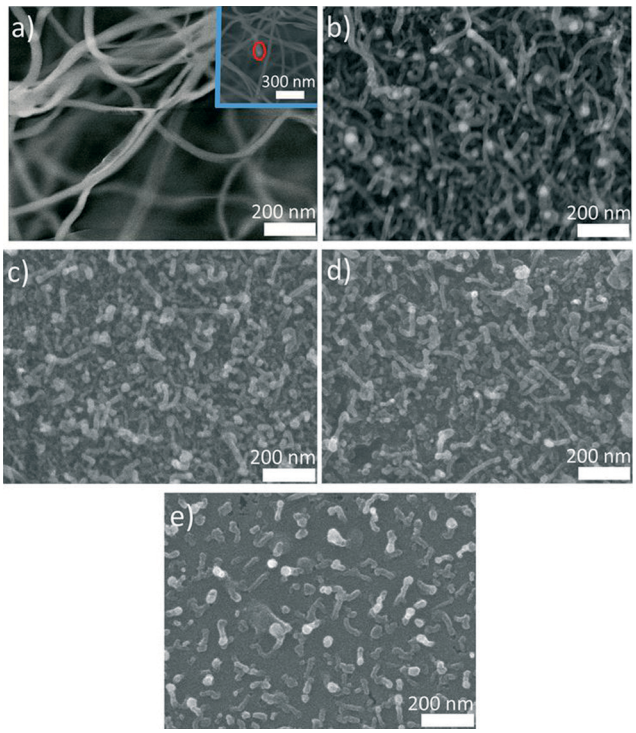

Fig. 1 SEM micrographs of silica nanowires grown under different conditions: (a) Ar atmosphere (the inset shows a PtSi nanoparticle on the tip of a nanowire), (b) dynamic vacuum at 10^{-3} torr, (c) sealed tube, 10^{-1} torr, (d) sealed tube, 10^{-2} torr, and (e) sealed tube, 10^{-3} torr.

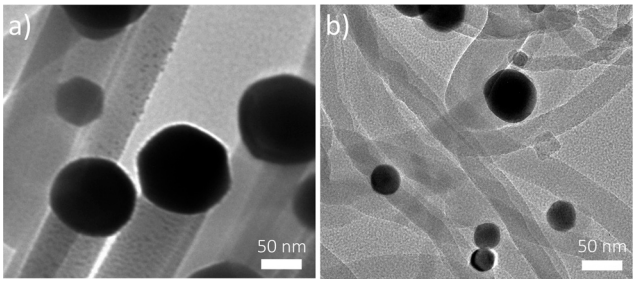

Fig. 2 TEM micrographs of silica nanowires grown under different conditions: (a) Ar atmosphere and (b) dynamic vacuum at 10^{-3} torr.

Elemental mapping by energy-dispersive X-ray (EDX) spectroscopy of the silica nanowires grown in Ar was performed with a scanning transmission electron microscope (STEM), as shown in Fig. 4. Different colours indicate the presence of different elements. It is seen that the nanoparticle on the tip consists of Pt and Si, and the nanowire is composed of Si and O. Notice that the oxygen does not spread uniformly, which indicates that oxidation of silica nanowires in Ar is rather chaotic and an uncontrolled process. The presence of mixed platinum and silicon signals on the tip of the nanowire can be explained as follows. As the silicon wafer was covered with Pt nanoparticles, the interdiffusion of Pt and Si during thermal annealing resulted in the formation of PtSi through the intermediate phase Pt_3Si. When the reaction continued to proceed, it would completely transform into PtSi.[25,26]

The compositional analysis by EDX (Table 1) confirms that the nanowires contain oxygen and silicon with a trace amount of platinum. The growth of nanowires in argon is

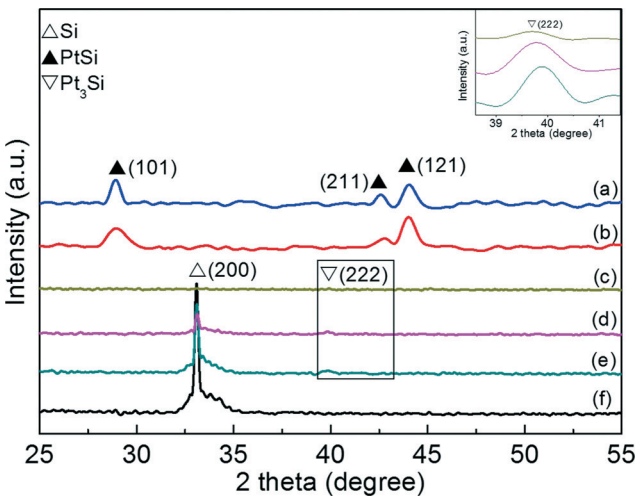

Fig. 3 XRD patterns of silica nanowires grown under various conditions: (a) argon, (b) dynamic vacuum, (c) sealed tube, 10^{-3} torr, (d) sealed tube, 10^{-2} torr, (e) sealed tube, 10^{-1} torr; and (f) XRD pattern of silicon substrate. The inset is an enlargement of the major peaks of Pt_3Si for samples annealed in sealed vacuum.

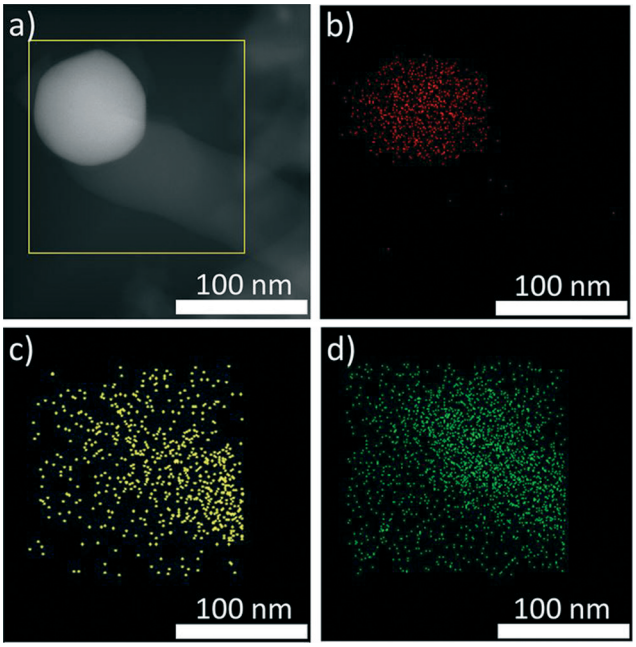

Fig. 4 (a) STEM image of a silica nanowire grown in argon flow and the corresponding EDX elemental mapping for elements (b) Pt, (c) O, and (d) Si.

Table 1 Chemical compositions (at%) of silica nanowires synthesized under different conditions by EDX analysis

Growth conditions	Si	O	Pt
Argon atmosphere	63.36	36.36	Balance
Vacuum, 10^{-3} torr	90.94	8.53	—
Sealed tube, 10^{-1} torr	89.25	10.55	—
Sealed tube, 10^{-2} torr	96.53	3.05	—
Sealed tube, 10^{-3} torr	97.55	1.57	—

determined by the well-defined VLS model, *i.e.*, the formation of Si vapour is activated through disproportionation and phase separation of volatile SiO vapour.[17–19] The nature of volatile SiO vapour is still under discussion and mostly speculative.[27–29] However, it is believed that active oxidation, controlled by the small partial pressure of oxygen in Ar, is responsible for the growth of silicon/silicon oxide nanowires.[19] The active oxidation process is explained by two sequential reactions: (1) $Si(s) + O_2(g) \rightarrow SiO_2(s)$ and (2) $Si(s) + SiO_2(s) \rightarrow 2SiO(g)$. At high temperature and low oxygen pressure, the active oxidation of silicon is the dominant reaction.[20] If the partial pressure of oxygen involved in the reaction is too high, the active oxidation process is terminated in reaction (1) and simply leads to the growth of a passivated SiO_2 layer.[30]

Most of the studies on active oxidation were conducted under UHV conditions.[31,32] However, a similar phenomenon was also observed for annealing in commercial gases, in which the Si surface underwent etching and weight loss while producing volatile SiO.[33] Therefore, it is believed that commercially available "high purity" processing gases such as Ar may contain residual oxygen estimated to be 3–10 parts per million (ppm), comparable to that observed under UHV conditions.[19,20] There was a claim that it satisfied the "critical conditions required for active oxidation"[20] and could promote the growth of silica nanostructures. However, this statement is not acceptable due to two reasons:

1. A simple calculation shows that the concentration of residual oxygen in argon at 1 atm, for example, estimated to be 3–10 ppm, is equal to a partial pressure of around 2×10^{-3} to 8×10^{-3} torr.[34,35] This is easily achievable by utilizing a basic rotary pump even in the absence of flowing argon.

2. The thermodynamic model of active oxidation based on steady state thermochemical calculation is only applicable to a fixed volume of gaseous constituents and can hardly be adopted by the system with flowing atmosphere.[18] Therefore, this model cannot be used as a reference for the growth of silica nanowires.

Thus, although UHV conditions are of importance for the initiation of active oxidation, we also arrive at a conclusion that the presence of Ar atmosphere as a source of oxygen with a concentration approaching UHV conditions has been underestimated. Therefore, at elevated temperatures, the growth of silica nanowires can be readily induced even in medium vacuum.

Although it has been proposed that the carrier gas can transport SiO vapour to the reaction sites,[26,36,37] this hypothesis cannot be considered seriously. Gaseous SiO is generated from the silicon substrate where the catalytic nanoparticles, so-called "reaction sites", are located. Therefore, there is no need to transport SiO vapour anywhere. Moreover, during the synthesis of silica nanowires the gas atmosphere usually flows in one direction. SiO vapour would be partially removed once it is generated from the silicon substrate. If the flow rate of Ar is too high, SiO would be removed completely, and the growth of nanowires can be suppressed.[38] It is important to note that the vapour transport mechanism is usually adopted only by systems with an additional source of SiO vapour, placed behind or in front of the silicon substrate covered by a catalyst. Once it evaporates, the gaseous species is directly transported by ambient flow to the reaction sites on the silicon substrate.[39,40] Furthermore, it is noticed that the growth of nanowires by other mechanisms (SLS or SSL) is also performed mostly in gas atmosphere.[41,42] As a result, the role of the carrier gas as the main factor in determining the growth of nanowires by the VLS mechanism is very speculative and needs more study. Continuous effort is needed to clarify this.

3.2. Thermal treatment in dynamic vacuum

The SiO_x nanowires grown in a dynamic vacuum of 10^{-3} torr (*i.e.*, in air flow with reduced pressure) possess a very compact morphology much different from that of the nanowires grown in Ar gas atmosphere, as seen in another SEM image (Fig. 1(b)). There are densely twisted nanowires, and it is

hard to distinguish individual nanowires. The diameter of the nanowires is 20–30 nm and the length is 2–3 μm. The tip of the nanowires is also covered with a nanoparticle, which can again be attributed to VLS growth (Fig. 2(b)). XRD analysis (Fig. 3(b)) shows that the nanowires also exhibit an amorphous structure, but three main peaks ascribed to PtSi particles are observed. This implies that the formation mechanism of the silica nanowires is the same as that of the nanowires grown in argon.

Elemental mapping (Fig. 5) demonstrates the distributions of Pt, O, and Si in the nanowires. Again, the nanoparticle on the tip of each nanowire is composed of Pt and Si, and the nanowire contains only Si and O. The intensity of the O signal in the nanowire is almost balanced with that of Si, and the silicon signals spread much more uniformly and consistently than those in Fig. 4. It implies that oxidation in dynamic vacuum is a more controllable process.

From EDX compositional analysis (Table 1), it can be seen that the nanowires contain less oxygen than those grown in argon. It is speculated that the nanowires comprise a silicon core that is grown at the beginning and later is partially oxidized to form SiO_x due to continuous exposure to residual oxygen at higher temperatures by disproportionation of SiO vapour. This architecture and the synthesis pathway are common for the disproportionation reaction of volatile SiO when the growth of nanowires is promoted by the VLS mechanism,[26,28,39] and might also be explained by the active oxidation model.[19,20] The extent of oxidation in the silicon nanowires and therefore the amount and thickness of silicon oxide are dependent on the degree of vacuum.

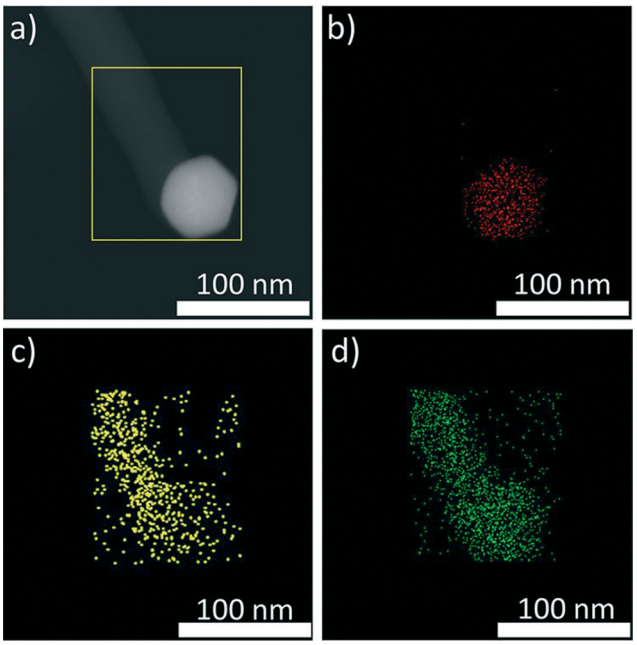

Fig. 5 (a) STEM image of a silica nanowire grown in dynamic vacuum and the corresponding EDX elemental mapping for elements (b) Pt, (c) O, and (d) Si.

The growth conditions and results follow the active–passive oxidation diagram (Fig. 6). The solid line represents the transition from stable passive oxidation to active oxidation. This line is derived from eqn (1) which expresses the critical conditions for SiO_2 growth (passive oxidation) in terms of critical oxygen pressure:[20,30]

$$P_c(T) = P_o \exp(-\Delta E/k_B T) \quad (1)$$

where P_o is 2×10^{12} torr, ΔE is 3.83 eV, T is temperature in Kelvin, and k_B is Boltzmann's constant. As can be seen from Fig. 6, the partial pressure of oxygen in a dynamic vacuum of 10^{-3} torr is approximately 2×10^{-4} torr (20% of 10^{-3} torr). This value is well below the transition line between passive and active oxidation. Thus, it is assumed that annealing in dynamic vacuum can easily initiate the formation of volatile SiO *via* the active oxidation process.

The range of the partial pressure of oxygen in flowing argon is shown as a vertical line in Fig. 6 for comparison. The difference in the partial pressures of residual oxygen in dynamic vacuum and in commercially available high purity Ar gas explains the dissimilarity of the results. It is obvious that annealing in argon produces more oxygen than that in dynamic vacuum at 10^{-3} torr, which almost immediately reacts with the newly grown silicon nanostructure to form an oxide. Oxidation usually starts from the external layer and gradually penetrates inside, altering the original silicon structure into silicon oxide. In the case of dynamic vacuum, partial oxidation takes place due to an insufficient amount of oxygen, resulting in lower oxygen content in the nanowires, as shown in Table 1. It is noted that the oxygen pressure in argon atmosphere is located in the passive oxidation region. The transition line in Fig. 6, however, is obtained based on a closed system,[20,30] which is different from the case of flowing

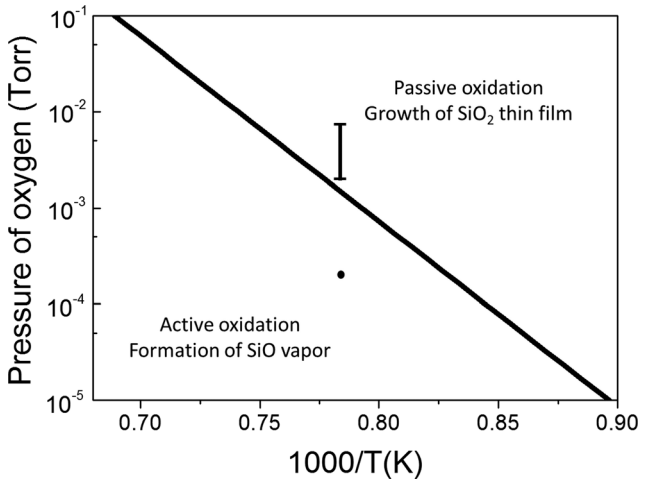

Fig. 6 Active–passive oxidation transition regime of silicon as a function of oxygen pressure and temperature taken from ref. 30. Vertical line: the oxygen partial pressure in argon atmosphere; solid dot: the oxygen partial pressure in dynamic vacuum (10^{-3} torr).

atmosphere. Furthermore, recent studies have demonstrated that the commonly accepted pressure of oxygen for active oxidation may be several orders of magnitude above the transition line for passive oxidation.[43] This would support our observation that the growth of nanowires in flowing argon is, in effect, by means of active oxidation.

3.3. Thermal treatment in sealed vacuum

In addition to residual oxygen in Ar or dynamic vacuum, it is intriguing to find out what would happen if oxygen is only present with a limited amount in a closed system. The following series of results are a first attempt to reveal it. Fig. 1(c)–(e) show the SEM images of the samples heated in a sealed vacuum tube. At 10^{-1} and 10^{-2} torr, the nanowires are both 20–30 nm in diameter and approximately 100 nm in length, but the number of nanowires at 10^{-2} torr is slightly smaller. By increasing the degree of vacuum to 10^{-3} torr, the length of the nanowires decreases dramatically. Moreover, the density of the nanowires also substantially decreases. This phenomenon seems to contradict the active oxidation mechanism, in which low pressure and high temperature are more favourable for synthesis of silica nanowires. However, this result confirms rather than denies that active oxidation is a main mechanism for the growth of silica nanowires. This phenomenon will be explained subsequently.

The nanoparticles on the tip of the nanowires can also be seen clearly from the SEM images, which again can be attributed to the VLS mechanism. The structure and phase of the nanowires were determined by XRD analysis. From Fig. 3, the XRD patterns of the samples have a clear peak at 33°, representing the Si (200) plane.[44] The peak is stronger for the samples grown in vacuum at 10^{-1} torr and much weaker for those grown at 10^{-3} torr. They are different from those prepared in flowing Ar and dynamic vacuum, implying that the nanowires are not completely oxidized and possess some amount of crystalline Si. The silica nanostructures can be identified according to the theory mentioned above as a core/shell structure in which the shell is amorphous silicon oxide and the core is silicon, or as partially oxidized crystalline Si nanowires. The XRD pattern in Fig. 3 reveals that the nanoparticles on the tip of the nanowires are Pt_3Si which is different from the samples annealed in argon and dynamic vacuum where PtSi was observed. It was proposed previously that the reaction between Si and Pt depends on the oxide layer formed on the surface of the silicon substrate.[45,46] The thicker the oxide layer, the less the direct contact of Pt with silicon is, thus the reaction between the Pt nanoparticles and the silicon substrate becomes more limited. Given the fact that the thicknesses of the oxide layer of the samples annealed in sealed tubes are smaller than those of the samples annealed in argon and dynamic vacuum,[47,48] the reaction between Si and Pt should lead to the complete formation of PtSi through the intermediate phase Pt_3Si. Yet, the obtained results challenge this argument. This phenomenon might be explained as follows.

By raising the temperature of annealing in sealed tubes, the oxide layer on the surface of silicon begins to grow. Since the sealed tubes cannot provide additional supply of oxygen, the increase in oxide layer thickness results in a gradual decrease in the concentration of oxygen. Meanwhile, the reaction between the silicon substrate and Pt nanoparticles also begins to proceed. At a certain temperature the reduced partial pressure of oxygen meets the conditions for desorption of the oxide layer by reaction (2) according to the active–passive oxidation diagram (Fig. 6). The temperature of transition between active and passive oxidation depends on the amount of available oxygen in the sealed tubes: the higher the degree of vacuum, the lower the temperature of transition. As a result, the sealed tubes become filled with gaseous SiO which almost immediately disproportionates into Si and SiO_2. Further reaction of Si with catalyst nanoparticles leads to the growth of silicon nanowires whose surface is instantly oxidized to SiO_x. Bearing in mind that the starting temperature of the growth of silicon nanowires for samples annealed in sealed tubes is lower than that for samples annealed in argon or dynamic vacuum, it can be assumed that Pt nanoparticles could only transform into the intermediate phase Pt_3Si before they are physically separated from the silicon substrate and situated on the tips of the nanowires. The further reaction between Pt and Si might be terminated due to the absence of a contact surface. Moreover, since the thickness of the oxide layer grown on the Si substrate is dependent on the amount of available oxygen in sealed tubes, it is evident that at lower levels of vacuum the reaction between Si and Pt becomes more limited. It would result in the appearance of less completely reacted phase Pt_3Si.

The Pt–Si binary phase diagram[49] confirms the existence of an intermediate compound that "consists of Pt_3Si and Pt", so-called $Pt_{25}Si_7$ (ref. 50 and 51). The formation of Pt-rich Pt_3Si as a first step of the Pt/SiO_2 interaction was also verified for the annealing in hydrogen and ascribed to "reduction of SiO_2 accompanied by the migration of Si atoms into the Pt particles".[52] With higher levels of vacuum in the sealed tube, the amount of the Pt-rich phase in the nanoparticles begins to decrease with increasing ratio of Si which would lead to a shift to lower angles of the (222) plane of Pt_3Si,[51,53] as can be seen from the inset in Fig. 3.

The EDX compositional analysis in Table 1 shows that the nanowires are composed mostly of silicon with a small amount of oxygen. The amount of oxygen depends on the level of vacuum. The higher the level of vacuum inside the sealed tube, the smaller the amount of oxygen in the nanowires is. This trend is common for silica nanostructures grown by the VLS mechanism,[28] and can be correlated with the growth of the oxide shell around the Si core, or limited oxidation of the Si nanowires.

In fact, the reduction of the partial pressure of oxygen, which is initially at 2×10^{-4} torr in a sealed vacuum of 10^{-3} torr, leads to gradual termination of the nanowire synthesis route. It is noted that the nanowires grown in the sealed tube at 10^{-3} torr could hardly be called "nanowires"

because the aspect ratio is too small. This also predicts that nanowires cannot be grown successfully under UHV conditions because of insufficient supply of oxygen, and it contradicts the theory of active oxidation for the silicon substrate where a low oxygen pressure inevitably causes the formation of volatile SiO and consequent growth of silica nanowires. It is therefore necessary to develop a new formation mechanism for silica nanowires to explain this result.

It is proposed that the growth of nanowires in sealed vacuum occurs *via* a modified active oxidation model, which allows the growth of nanowires even in medium or low vacuum. In a sealed tube the role of reaction (1) is more predominant initially, and it influences much of the whole growth process. During the evolution of a passive layer, the amount of oxygen in the sealed tube gradually decreases to a value suitable for promoting the active oxidation reaction. Volatile SiO(g) is generated by reaction (2) through the desorption of the oxide layer.[54] It is obvious that the amount of SiO, which later disproportionates to produce Si, is directly dependent on the amount of silicon dioxide grown on the surface of silicon. For the case of 10^{-3} torr, the thickness of silicon dioxide is much smaller than those for 10^{-1} torr and 10^{-2} torr, and the oxide grows at a much slower rate. The nanowires grown at 10^{-3} torr would finally consume all available SiO vapour. As a result, the growth of nanowires is terminated, resulting in a smaller length. Due to the very low concentration of oxygen after the active oxidation process is initiated, oxidation of Si nanowires would be very limited. Even for the sealed tube at 10^{-1} torr where the length of nanowires is the longest, the amount of oxygen cannot oxidize all of them uniformly due to an insufficient quantity.

Conclusions

The growth of silicon/silicon oxide nanowires under different conditions was studied. It was demonstrated that silica nanowires could be grown in environments with various concentrations of oxygen in flowing gas or without a continuous supply of oxygen. The partial pressure and amount of oxygen were crucial to influence the final morphology and composition of the nanostructures. For nanowires grown without a continuous supply of oxygen, the lower the oxygen partial pressure, the shorter and less dense they are. For nanowires grown with a continuous supply of oxygen, the higher the oxygen pressure, the longer and larger the nanowires are.

Acknowledgements

This work was supported by the Ministry of Science and Technology of Taiwan under contract no. NSC 99-2221-E-007-066-MY3 and NSC 101-2120-M-007-013. The authors express special thanks to Drs. M. Mishra and C.-C. Kei for thoughtful discussion and C.-Y. Su for SEM analysis.

Notes and references

1 P. Zhang and Y. Cui, *CrystEngComm*, 2013, **15**, 9963.
2 G. Bilalbegović, *J. Phys.: Condens. Matter*, 2006, **18**, 3829.
3 Y. Y. Choi, S. J. Park, Y. Kim and D. J. Choi, *CrystEngComm*, 2012, **14**, 5552.
4 D. P. Yu, Q. L. Hang, Y. Ding, H. Z. Zhang, Z. G. Bai, J. J. Wang, Y. H. Zou, W. Qian, G. C. Xiong and S. Q. Feng, *Appl. Phys. Lett.*, 1998, **73**, 3076.
5 G. Callsen, J. S. Reparaz, M. R. Wagner, A. Vierck, M. R. Phillips, C. Thomsen and A. Hoffmann, *Nanotechnology*, 2011, **22**, 405604.
6 M. Zhang, E. Ciocan, Y. Bando, K. Wada, L. L. Cheng and P. Pirouz, *Appl. Phys. Lett.*, 2002, **80**, 491.
7 X. C. Wu, W. H. Song, K. Y. Wang, T. Hu, B. Zhao, Y. P. Sun and J. J. Du, *Chem. Phys. Lett.*, 2003, **336**, 53.
8 K. W. Kolasinski, *Curr. Opin. Solid State Mater. Sci.*, 2006, **10**, 182.
9 R. S. Wagner and W. C. Ellis, *Appl. Phys. Lett.*, 1964, **4**, 89.
10 H. Luo, R. Wang, Y. Chen, D. Fox, R. O' Connel, J. J. Wang and H. Zhang, *CrystEngComm*, 2013, **15**, 10116.
11 Y. Choi, J. L. Johnson and A. Ural, *Nanotechnology*, 2009, **20**, 135307.
12 J. H. Hsu, M. H. Huang, H. H. Lin and H. N. Lin, *Nanotechnology*, 2006, **17**, 170.
13 M. N. Banis, Y. Zhang, R. Li, X. Sun, X. Jiang and D. Nikanpour, *Particuology*, 2011, **9**, 458.
14 H. W. Kim, S. H. Shim and J. W. Lee, *Phys. E*, 2007, **37**, 163.
15 Y. W. Wang, C. H. Liang, G. W. Meng, X. P. Peng and L. D. Zhang, *J. Mater. Chem.*, 2002, **12**, 651.
16 L. Dai, L. P. You, X. F. Duan, W. C. Lian and G. G. Qin, *Phys. Lett. A*, 2005, **335**, 304.
17 R. G. Elliman, T. H. Kim, A. Shalav and N. H. Fletcher, *J. Phys. Chem. C*, 2012, **116**, 3329.
18 Y. Yang, A. Shalav, T. Kim and R. G. Elliman, *Appl. Phys. A: Mater. Sci. Process.*, 2012, **107**, 885.
19 T. H. Kim, A. Shalav and R. G. Elliman, *J. Appl. Phys.*, 2010, **108**, 076102.
20 A. Shalav, T. Kim and R. G. Elliman, *IEEE J. Quantum Electron.*, 2011, **17**, 785.
21 E. K. Lee, B. L. Choi, Y. D. Park, Y. Kuk, S. Y. Kwon and H. J. Kim, *Nanotechnology*, 2008, **19**, 185701.
22 T. X. Nie, Z. G. Chen, Y. Q. Wu, J. L. Wang, J. Z. Zhang, Y. L. Fan, X. J. Yang, Z. M. Jiang and J. Zou, *J. Phys. Chem. C*, 2010, **114**, 15370.
23 J. Niu, J. Sha, Z. Liu, Z. Su, J. Yu and D. Yang, *Phys. E*, 2004, **24**, 268.
24 H. W. Kim, S. H. Shim, M. H. Kong and H. H. Yang, *Phys. Status Solidi A*, 2008, **205**, 2002.
25 J. Drobek, R. C. Sun and T. C. Tison, *Phys. Status Solidi A*, 1971, **8**, 243.
26 P. K. Sekhar, S. N. Sambandam, D. K. Sood and S. Bhansali, *Nanotechnology*, 2006, **17**, 4606.
27 J. H. Song, D. H. Lim, E. S. Oh, M. H. Cho, J. P. Ann, J. G. Kim, H. C. Sohn and D. H. Ko, *J. Korean Phys. Soc.*, 2010, **57**, 1467.
28 F. M. Kolb, A. Berger, H. Hofmeister, E. Pippel, U. Gösele and M. Zacharias, *Appl. Phys. Lett.*, 2006, **89**, 173111.
29 R. Esterina, X. M. Liu, C. A. Ross, A. O. Adeyeye and W. K. Choi, *J. Appl. Phys.*, 2012, **112**, 024312.

30 F. W. Smith and G. Ghidini, *J. Electrochem. Soc.*, 1982, **129**, 1300.
31 J. R. Engstrom, D. J. Bonser, M. M. Nelson and T. Engel, *Surf. Sci.*, 1991, **256**, 317.
32 T. Engel, *Surf. Sci. Rep.*, 1993, **18**, 91.
33 C. J. Frosch and L. Derick, *J. Electrochem. Soc.*, 1957, **104**, 547.
34 F. H. Lu and H. Y. Chen, *Thin Solid Films*, 1999, **355–356**, 374.
35 C. Y. Wang, L. H. Chan, D. Q. Xiao, T. C. Lin and H. C. Shih, *J. Vac. Sci. Technol., B*, 2006, **24**, 613.
36 D. K. Sood, P. K. Sekhar and S. Bhansali, *Appl. Phys. Lett.*, 2006, **88**, 143110.
37 J. L. Elechiguerra, J. A. Manriquez and M. J. Yacaman, *Appl. Phys. A: Mater. Sci. Process.*, 2004, **79**, 461.
38 M. S. Al-Ruqeishi, R. M. Nor, Y. M. Amin and K. Al-Azri, *Silicon*, 2010, **2**, 19.
39 F. M. Kolb, H. Hofmeister, R. Scholz, M. Zacharias, U. Gösele, D. D. Ma and S. T. Lee, *J. Electrochem. Soc.*, 2004, **151**, G472.
40 Z. W. Pan, Z. R. Dai, L. Xu, S. T. Lee and Z. L. Wang, *J. Phys. Chem. B*, 2001, **105**, 2507.
41 H. F. Yan, Y. J. Xing, Q. L. Hang, D. P. Yu, Y. P. Wang, J. Xu, Z. H. Xi and S. Q. Feng, *Chem. Phys. Lett.*, 2000, **323**, 224.
42 D. P. Yu, Y. J. Xing, Q. L. Hang, H. F. Yan, J. Xu, Z. H. Xi and S. Q. Feng, *Phys. E*, 2001, **9**, 305.
43 J. V. Seiple and J. P. Pelz, *J. Vac. Sci. Technol., A*, 1995, **13**, 772.
44 W. Zhang, L. Guo, G. Peng, T. Li, S. Feng, Z. Zhou, T. Peng and Z. Quan, *Thin Solid Films*, 2011, **520**, 769.
45 C. A. Chang, A. Segmüller, H. C. W. Huang, F. E. Turene, B. Cunningham and P. A. Totta, *J. Vac. Sci. Technol., A*, 1986, **4**, 841.
46 C. Harder, L. Hammer and K. Müller, *Phys. Status Solidi A*, 1994, **146**, 385.
47 Y. Enta, B. S. Mun, M. Rossi, P. N. Ross Jr., Z. Hussain, C. S. Fadley, K. S. Lee and S. K. Kim, *Appl. Phys. Lett.*, 2008, **92**, 012110.
48 K. Kawamura and T. Motooka, *J. Electrochem. Soc.*, 2006, **153**, G1078.
49 H. Okamoto, *J. Phase Equilib.*, 1995, **16**, 286.
50 A. Gribanov, A. Grytsiv, E. Royanian, P. Rogl, E. Bauer, G. Giester and Y. Seropegin, *J. Solid State Chem.*, 2008, **181**, 2964.
51 R. Massara and P. Feschotte, *J. Alloys Compd.*, 1993, **201**, 223.
52 D. Wang, S. Penner, D. S. Su, G. Rupprechter, K. Hayek and R. Schlögl, *J. Catal.*, 2003, **219**, 434.
53 A. A. Permyakova, N. J. Bjerrum, J. O. Jensen and Q. Li, *PhD thesis*, DTU Energy Conversion, 2013.
54 Y. S. Lai, J. L. Wang, S. C. Liou and C. H. Tu, *Chem. Phys. Lett.*, 2008, **453**, 97.

